The Journal of Chemical Physics

RESEARCH ARTICLE | FEBRUARY 11 2025

Ionic association and Wien effect in 2D confined electrolytes

Damien Toquer ; Lydéric Bocquet ; Paul Robin

J. Chem. Phys. 162, 064703 (2025)
https://doi.org/10.1063/5.0241949

The Journal of Chemical Physics ARTICLE pubs.aip.org/aip/jcp

Ionic association and Wien effect in 2D confined electrolytes

Cite as: J. Chem. Phys. 162, 064703 (2025); doi: 10.1063/5.0241949
Submitted: 1 October 2024 • Accepted: 17 January 2025 •
Published Online: 11 February 2025

Damien Toquer,[1] Lydéric Bocquet,[1,a)] and Paul Robin[2,b)]

AFFILIATIONS

[1] Laboratoire de Physique de l'École Normale Supérieure, ENS, Université PSL, CNRS, Sorbonne Université, Université Paris Cité, Paris, France
[2] Institute of Science and Technology Austria, Am Campus 1, 3400 Klosterneuburg, Austria

[a)] Electronic mail: lyderic.bocquet@ens.fr
[b)] Author to whom correspondence should be addressed: paul.robin@ist.ac.at

ABSTRACT

Recent experimental advances in nanofluidics have allowed to explore ion transport across molecular-scale pores, in particular, for iontronic applications. Two-dimensional nanochannels—in which a single molecular layer of electrolyte is confined between solid walls—constitute a unique platform to investigate fluid and ion transport in extreme confinement, highlighting unconventional transport properties. In this work, we study ionic association in 2D nanochannels, and its consequences on non-linear ionic transport, using both molecular dynamics simulations and analytical theory. We show that under sufficient confinement, ions assemble into pairs or larger clusters in a process analogous to a Kosterlitz–Thouless transition, here modified by the dielectric confinement. We further show that the breaking of pairs results in an electric-field dependent conduction, a mechanism usually known as the second Wien effect. However the 2D nature of the system results in non-universal, temperature-dependent, scaling of the conductivity with electric field, leading to ionic coulomb blockade in some regimes. A 2D generalization of the Onsager theory fully accounts for the non-linear transport. These results suggest ways to exploit electrostatic interactions between ions to build new nanofluidic devices.

I. INTRODUCTION

Recent years have witnessed critical advances in the fabrication of atomic-scale fluidic channels[1–7] in an effort to achieve molecular control over water and ion transport—similar to the transport machinery of cells. Considering the intense complexity of such nano-fabrication techniques, theoretical guidance has become necessary; however, traditional continuous models of fluid and charge transport break down under such extreme confinement.[1,8–14]

Particular attention has been drawn to 2D nanochannels recently[6,15] [Fig. 1(a)]. These systems, which are fabricated by van der Waals assembly, consist in flakes of a 2D material (graphene, MoS_2, hBN...) separated by graphene ribbons, creating an atomically smooth and thin channel permeable to water. Electrolytes confined inside such structures are expected to form a single ionic layer, which has been shown to enhance electrostatic interactions between ions[10,14] and promote memory effects in conduction, such as the recently demonstrated memristor effect.[13,14]

The properties of ions in such systems have been studied using various techniques, both in theory—mean field approaches[14,16] and exact field theories[17,18]—and in simulations—Brownian,[10,14] molecular,[14,19] or *ab initio* dynamics[19] and more recently machine learning forcefields trained with density functional theory (DFT)-generated datasets.[20] Overall, a growing body of evidence is shedding light on links between electrostatic correlations and non-linear ion transport.[21] A common blind spot of the aforementioned numerical approaches is the description of out of equilibrium ion transport. While theoretical predictions recently showed that 2D nanochannels should display non-linear conduction due to electrostatic interactions between ions, numerical evidence for this has remained scarce, in particular, due to the high computational cost of simulating large systems over long timescales.

In this work, we implement molecular dynamics simulations to carry out a full description of ion association in 2D nanochannels and show how electrostatic interactions impact charge transport at the molecular scale. We use a combination of Brownian

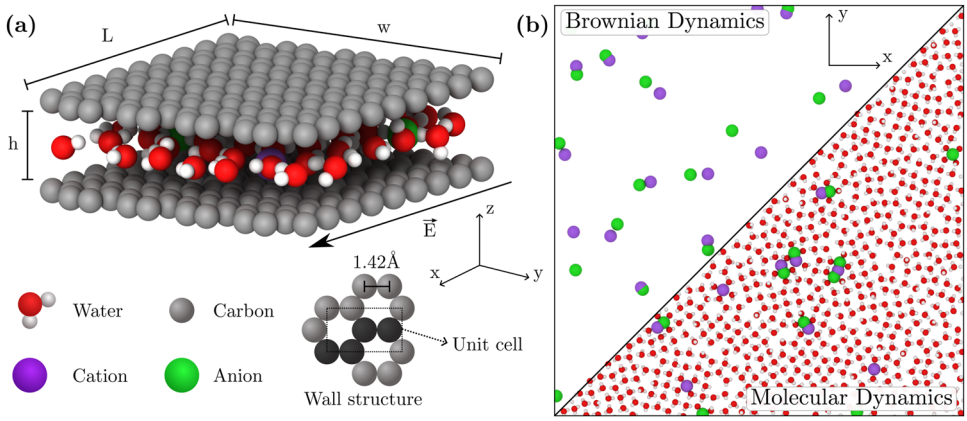

FIG. 1. System studied in this paper. (a) Simulation setup for the molecular dynamics simulation. The walls are generated from a unit cell of four carbon atoms, shown in black in the structure. (b) Comparison of Brownian dynamics (top left) and molecular dynamics (bottom right) simulations at the same ionic density.

dynamics (BD), where the solvent and channel walls are treated implicitly, and all-atom molecular dynamics (MD). The latter is particularly suited for identifying the impact of the discreteness of water molecules, while the former gives access to long-time dynamics by saving computational cost. We show that these two techniques offer complimentary tools to characterize ion association and ion–ion correlations in general. In both cases, we fully describe the formation of ionic clusters as a function of the relative strength of electrostatic interactions compared to thermal noise.

Simulations are complemented with an analytical framework of equilibrium and non-equilibrium properties, whose predictions are in excellent agreement with the numerical results.

This paper is organized as follows. In Sec. I, we describe our numerical implementation and how it can be used to quantify ionic pairing in confinement. Section II describes ionic association. We show how electrostatic correlations under confinement result in ionic pairing at thermal equilibrium, unveiling a transition between a fully paired state and a partially dissociated state as a function of temperature, similar to a modified Kosterlitz–Thouless transition. In Sec. III, we explore out-of-equilibrium properties and demonstrate non-linear transport of ions in the monolayer, governed by pair breaking under an electric field (a phenomenon known as the second Wien effect).

II. METHODS

In this work, we model an electrolyte confined in a 2D nanochannel of height h, made of carbon walls [Fig. 1(a)]. We assume that the system is connected to macroscopic fluidic reservoirs where Ag/AgCl electrodes are located, imposing a voltage drop across the system and creating a static electric field $\vec{E}$.

A. MD and BD dynamics

Two different simulation methods are used throughout this paper. In all-atom molecular dynamics (MD), the entire system [water molecules, ions, and atoms from the channel walls, see Fig. 1(a)] is simulated using classical Lennard–Jones and Coulombic forcefields and solving Newton's equations of motion. In Brownian dynamics (BD), on the other hand, water and channel walls are treated implicitly, and only the positions of ions are tracked using overdamped Langevin equations [Fig. 1(b)]. This is motivated by the finding that electrostatic interactions between ions from the walls and the solvent can be accounted for in a coarse-grained way by renormalizing the ion–ion interaction potential.[10] Further details regarding the simulation methodology can be found in the supplementary material.

B. Interaction potentials

In MD dynamics, as stated above, all particles (ions, wall atoms, and water molecules) interact both through electrostatic and Lennard–Jones interactions, the latter representing attractive and repulsive van der Waals forces. The interaction energy between particles i and j, thus, reads

$$V_{ij}(r) = 4\epsilon\left[\left(\frac{\sigma}{r}\right)^{12} - \left(\frac{\sigma}{r}\right)^{6}\right] + \frac{q_i q_j}{4\pi\epsilon_0 r}, \tag{1}$$

where q_i is the charge of particle i, r is the interparticle distance, and ϵ and σ are some particle-specific constants detailed in the supplementary material.

One of the main shortcomings of MD dynamics is that only a fraction of the simulation time is spent on simulating ion dynamics—the focus of this work. Integrating out solvent degrees of freedom allows to run much faster implicit-solvent BD simulations. This is usually done by modeling water as a dielectric medium of constant $\epsilon_w = 80$; however, here one must account for atomic confinement as well. Walls not only restrict ion transport geometrically but also modify the electric potentials generated by ions due to having a much lower permittivity compared to water (in what follows, we will assume that the walls have a dielectric constant $\epsilon_s = 2$)—this process, called interaction confinement,[10] is caused by the fact electric field lines from ions cannot fully penetrate the walls and instead concentrate within the fluid. Overall, this results in a renormalized ion–ion potential given by[10]

$$V_{ij}(r) = \frac{q_i q_j}{4\pi\epsilon_0\epsilon_w r}\int_0^\infty J_0(u)\frac{\tanh\left[u\frac{h}{2r}\right] + \frac{\epsilon_w}{\epsilon_s}}{\frac{\epsilon_w}{\epsilon_s}\tanh\left[u\frac{h}{2r}\right] + 1}, \tag{2}$$

where J_0 is a Bessel function and we recall that h is the height of the channel. For $\epsilon_w/\epsilon_s \gg 1$ and $r \gg h$, the above integrand can be

cut into $0 < u < A$ and $u > A$ [defined by $\int_0^A J_0(u)\,\mathrm{d}u = 0$, $A \simeq 1.1$]. Assuming that the latter part oscillates quickly and integrate to zero and that $\int_0^A J_0(u) \times [\ldots] \simeq \int_0^A \frac{1}{A} \times [\ldots]$, we obtain

$$\beta V_{ij}(r) = -\frac{\mathrm{sign}\,(q_i q_j)}{T^*} \log\left(\frac{r}{r+\xi}\right), \tag{3}$$

where we introduced the inverse temperature β as well as two other parameters: the dielectric length,

$$\xi = A\epsilon_w h/2\epsilon_s, \tag{4}$$

and the (dimensionless) reduced temperature T^* defined by,

$$T^* = \frac{2\pi\varepsilon_0\varepsilon_w h}{Z^2 e^2 A} k_B T, \tag{5}$$

with Z being the valency of ions and e being the elementary charge. This parameter plays the role of a coupling constant; we will use it throughout this manuscript as a measure of the strength of electrostatic interactions. One finds that $T^* \simeq 0.4$ for monovalent ions at room temperature and $T^* \simeq 0.1$ for divalent ions. In practice, we use this potential in BD simulations, with $\xi \simeq 14$ nm. It should be noted that in the limit $r \ll \xi$, one recovers $V_{ij}(r) \simeq q_i q_j/4\pi\epsilon_0\epsilon_s r$ as field lines now fully permeate the solid.

When comparing with MD simulations, one should note that the system is confined between two vacuum slabs (as walls are made of a single layer of carbon atoms), corresponding to $\epsilon_s = 1$ and $\xi \simeq 28$ nm. Throughout this paper, to simplify discussion, we always assume that $Z = 2$, and we instead use temperature as a tuning parameter of the interactions.

Confinement has been shown to reduce the effective permittivity of water or make it anisotropic.[22–24] The exact dielectric properties of confined water are still debated, however, with some recent experiments showing an increase in in-plane permittivity instead.[25] It has been shown elsewhere[14] that dielectric anisotropy only has a weak effect on ion–ion interactions. In addition, our results can be extended in a straightforward way to other values of ϵ_w in confinement by tuning T^*.

Finally, while in this paper we only consider the case of non-conducting walls made of a dielectric material, the impact of wall conductivity has been discussed elsewhere.[10,26,27] Briefly, conduction electrons within the walls are able to screen off ion–ion electrostatic interactions, reducing their range.

C. Ionic current

For a given value of the imposed electric field $\vec{E}$, we extract the ionic current density from simulated trajectories through

$$j = Ze\frac{N}{h\mathcal{A}}(\langle v_+\rangle - \langle v_-\rangle), \tag{6}$$

where $\langle v_+\rangle$ and $\langle v_-\rangle$ are, respectively, the time-averaged velocity of the cations and the anions along the direction of the field, N is the number of ions, and $\mathcal{A}$ is the 2D area spanned by the channel. We can deduce the conductivity through

$$\sigma(E) = \frac{j(E)}{E}, \tag{7}$$

which we will compare to the Ohmic conductance (defined for ions behaving like ideal tracer particles),

$$\sigma_0 = \frac{2N}{h\mathcal{A}}\frac{(Ze)^2 D}{k_B T}, \tag{8}$$

with D being the diffusion coefficient of ions, assumed to be the same for anions and cations (in the case of a difference in diffusivity, D should be replaced by the average of the coefficients of cations and anions). Parameters of BD simulations are chosen so that $D/k_B T$ is independent of temperature so that we can use the same value of σ_0 to compare the conductivity of the system for different strengths of electrostatic interactions.

D. Ionic pairs and clusters

We observe in BD simulations that at low temperature, ions tend to form pairs. Since they are neutral and do not contribute to conduction, we use conductivity measurements as a way of quantifying the fraction of free ions n_f,

$$n_f = \frac{\sigma(E)}{\sigma_0}. \tag{9}$$

This definition of ionic pairing has the advantage of being the closest to what could be measured in experiments, in addition to being very convenient to compute. In fact, it effectively counts the fraction of charge carriers only if we can neglect higher-order correlations between ions (which tend to impede conduction compared to the Ohmic case) or, equivalently, if we assume the mobility of individual ions not to vary with the field. We make this assumption in the following since we expect the non-linearity of the system to be dominated by the variation of the fraction of charge carriers (second Wien effect) and not by the variation of the mobility (first Wien effect[28,29] and Debye–Hückel correlations in general[30]). This intuitive definition unfortunately fails if E is too low due to a poor signal-to-noise ratio. In the supplementary material, we report an alternative definition based on correlation functions, which is consistent with Eq. (9) but can be extended without problem to $E = 0$.

In MD simulations, we observe the formation of large ionic clusters, in addition to ionic pairing. Some of these clusters bear a non-zero charge and, therefore, participate to conduction. We, therefore, distinguish between two quantities: first, the fraction n_f of free ions and the fraction of charged clusters n_f^{cluster} (which includes free ions—as they are charged clusters of size 1). In practice, we find that all clusters containing an even number of ions are electrically neutral, and odd-sized clusters have a charge ±1 (as clusters with multiple charge defects are highly unstable). From there, we can deduce that a measure of the fraction of charge carriers density is

$$n_f^{\mathrm{cluster}} = \frac{\sum_{l\,\mathrm{odd}} N_l}{2N}, \tag{10}$$

with N_l being the number of clusters of size l, which we determine directly from trajectories through network analysis. The fraction of free ions is defined as

$$n_f = \frac{N_1}{2N}. \tag{11}$$

This exact procedure used to compute N_l from trajectories is described in the supplementary material.

III. PAIRING TRANSITION AND ELECTROSTATIC SCREENING

In this section, we quantify the formation of ionic pairs using both simulations and theoretical analysis. We start by predicting that the system undergoes a conductor/insulator phase transition reminiscent of the 2D Kosterlitz–Thouless transition. We analytically predict the system's critical temperature, which is found to slightly deviate from the usual KT result due to the quasi-2D nature of confined electrolytes. We then compare those results to simulations. We find that indeed at low temperature, almost all ions assemble into pairs. We characterize this transition numerically and show it is of infinite order as predicted by the KT analogy.

A. Theoretical analysis

1. Critical temperature and correlation length

It has been shown[16] that the 2D Coulomb gas, made of charged particles interacting through a potential $V(r) = -\frac{1}{T^*}\log r$, undergoes a pairing phase transition for $T^* < 0.25$ that is equivalent to the Kosterlitz–Thouless transition. Here, we sketch the outline of such a derivation while focusing on differences between the exact 2D Coulomb gas and our actual system—2D confined electrolytes.

At the mean-field level, we can treat ion pairs as a separate, ideal chemical species and write down the chemical equilibrium with free ions,

$$n_p = 1 - n_f = \zeta n_f^2 e^{2\beta\mu_e}. \tag{12}$$

Here, n_p is the fraction of ions that are part of a pair, n_f is the free ion fraction, μ_e is the excess chemical potential of free ions, $\beta = 1/k_B T$, and ζ is the internal partition function of a pair. In the 2D Coulomb gas, μ_e can be obtained through a Debye charging process by computing the field created on a given ion by its surrounding Debye atmosphere,

$$2\beta\mu_e = \frac{1}{T^*}\left[\frac{K_0(\kappa_D r_0)}{\kappa_D r_0 K_1(\kappa_D r_0)}\right], \tag{13}$$

where r_0 is a measure of the ionic size, K_0 and K_1 are modified Bessel functions of the second kind, and

$$\kappa_D = \sqrt{\frac{4\pi n_f c}{T^*}} \tag{14}$$

is the inverse Debye length at salt concentration c (expressed in atoms per surface area). For $T^* < T_c^* = 0.25$, Eq. (12) becomes $1 - n_f \propto n_f^{2-1/2T^*}$, with $2 - 1/2T^* < 0$, and, therefore, admits no solution. This is the signature of the pairing transition. In addition, just above the transition, one can compute the correlation length through the Debye length (in the limit where the salt concentration is not too high[31]),

$$\lambda_D = \sqrt{\frac{T^*}{4\pi n_f c}} \underset{T^* \to T_c^*}{\propto} e^{\frac{T^*/4}{T^* - T_c^*}}. \tag{15}$$

The correlation length, therefore, depends in a non-algebraic manner on temperature, and in particular, no critical exponent can be defined—this shows that the phase transition is of infinite order. Interestingly, the system possesses a critical *line*, meaning that there is a single value of the phase transition temperature regardless of salt concentration. This line ends at a given value of concentration, depending on the precise value of ζ and the exact criterion used to define ion pairs (for our choice of parameters, the transition occurs independently of concentration for $c < 0.9$M).

In our case, however, ionic interactions are not exactly logarithmic: $V(r) \sim -\frac{1}{T^*}\log r/(r+\xi)$ [see Eq. (3)]. Repeating the above argument, we find that

$$2\beta\mu_e = \frac{1}{T^*}\left[\frac{\xi}{\kappa_D r_0 (r_0+\xi)}\frac{K_0(\kappa_D r_0) - K_0(\kappa_D (r_0+\xi))}{K_1(\kappa_D r_0) - K_1(\kappa_D (r_0+\xi))}\right]. \tag{16}$$

Then, Eq. (12) stops having a solution for

$$T_c^* = -\frac{1}{4}\frac{\xi}{\xi+1}\min_k k\frac{\partial g_\xi}{\partial k}, \tag{17}$$

where we defined

$$g_\xi(k) = \frac{K_0(k) - K_0(k(1+\xi/r_0))}{K_1(k) - K_1(k(1+\xi/r_0))}. \tag{18}$$

We notably find that $T_c^* \simeq 0.18$ for $\xi/r_0 = 14$, and we recover $T_c^* = 1/4$ for $\xi \to \infty$.

Finally, let us discuss the case where the dielectric length ξ is short, such as for $\epsilon_s \sim \epsilon_w$. In that case, interactions are weakened as the electric field lines of ions leak into the walls. This situation is similar to confinement by conducting or metallic walls.[10,26,27] While some degree of ionic pairing was reported in such context, it is *a priori* much weaker than for channels with high dielectric contrast, such as here.

2. Discussion and scaling laws

In the previous paragraph, we discussed the formation of ion pairs in confined electrolytes. These pairs, called Bjerrum pairs, are usually absent from bulk aqueous electrolytes; we, thus, discuss the impact of confinement below.

In any setting, the strength of the ionic interactions can be quantified by the Bjerrum length[32] l_B, defined as

$$\beta V(\ell_B) = k_B T. \tag{19}$$

It is the typical length at which electrostatic interactions become comparable to thermal agitation. For a bulk system, the Bjerrum length is then given by

$$\ell_B^{\text{bulk}} = \frac{e^2}{4\pi\epsilon_0\epsilon_w k_B T}, \tag{20}$$

while for a 2D confined electrolyte, where electrostatic interactions are quasi-logarithmic [see Eq. (3)], it reads

$$\ell_B^{\text{2D}} = \frac{\xi}{e^{T^*} - 1} \sim \frac{\xi}{T^*}. \tag{21}$$

This can be used to compare the interaction in each systems,

$$\frac{\ell_B^{2D}}{\ell_B^{bulk}} \simeq \frac{\varepsilon_w}{\varepsilon_s} \gg 1. \tag{22}$$

This notably shows how, under confinement, dielectric contrast between the walls and water greatly reinforces electrostatic interactions. In bulk water, $\ell_B^{bulk} = 0.7$ nm, meaning that long-range interactions between ions are essentially negligible compared to thermal noise. In the slit, this is not the case anymore as the Bjerrum length is orders of magnitude larger: for our choice of parameters, we obtain $\ell_B = 14$ nm, far exceeding any other microscopic length scale. As we will discuss in several later points, 2D confined electrostatic interactions are nearly scale-invariant, owing to their quasi-logarithmic nature.

This fact allows us to understand the emergence of the phase transition using scaling laws. The excess chemical potential μ_e of free ions can be thought of as half the free energy cost of breaking a pair. Since the free cation and anion obtained by breaking a pair are on average distant by λ_D, we can assume that

$$2\beta\mu_e \sim \frac{1}{T^*} \log \lambda_D / r_0, \tag{23}$$

where r_0 is the ionic size. At low enough temperature, we expect that most ions are paired so that $n_p = 1 - n_f \simeq 1$. From the chemical equilibrium (12) and using the definition of λ_D, we obtain

$$n_f \propto c^{\frac{1}{4T^*-1}}. \tag{24}$$

This leads to a contradiction if $T^* < 0.25$: for low enough salt concentration c, $n_f > 1$, which is impossible—the chemical equilibrium is broken and there is a phase transition.

B. Comparison with simulations

1. Brownian dynamics simulations

In order to verify our theoretical results with our BD simulations, we plot in Fig. 2(a) the evolution of the free ion fraction with the reduced Coulomb temperature for $\xi = 13.8$ nm. As we lower the temperature, the free ion fraction decreases, up to an almost fully paired system for a finite value of temperature. Quantitatively, one can define the critical temperature in BD simulations as the temperature for which the system's correlation length diverges. In Fig. 2(a), we show the evolution of the Debye length λ_D with temperature, and we fit data from BD simulations with an ansatz inspired by Eq. (15) (solid blue line),

$$\lambda_D(T^*) \propto \exp\left[\frac{T^*/4}{T^* - T_c^*}\right]. \tag{25}$$

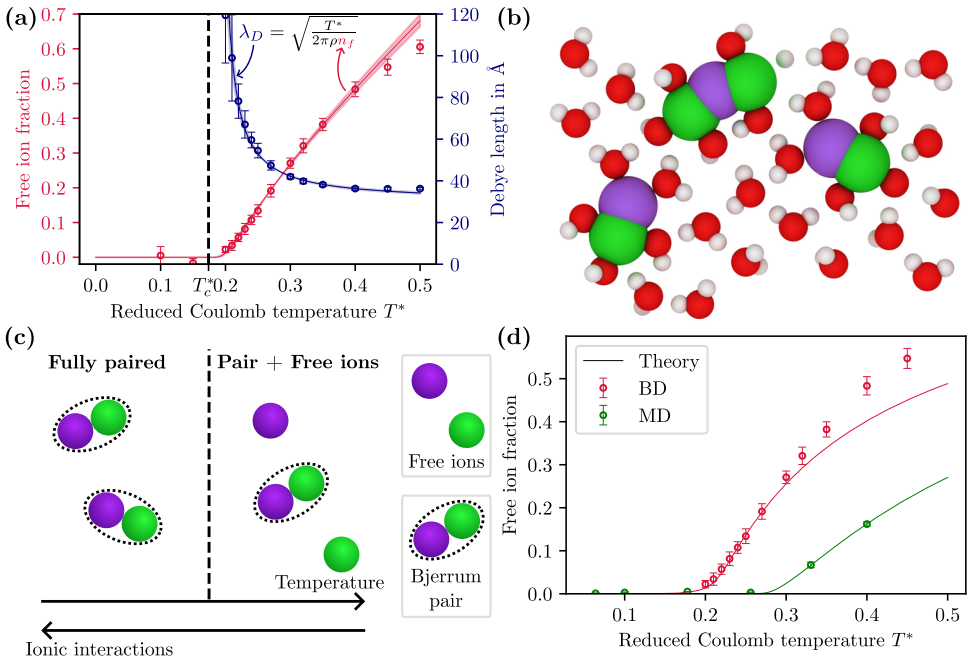

FIG. 2. Pairing transition in theory and simulations. (a) (Red points) Free ion fraction from BD simulation for various reduced Coulomb temperatures. (Red line) Fit of the free ion fraction for an infinite order phase transition. (Blue points and line) Debye length obtained from the free ion fraction using Eq. (15). (b) Screenshot from MD simulations at equilibrium for $T^* = 0.1$. We observe large ionic clusters (seven ions in the screenshot) that move together and can have a net charge (−1 in the screenshot). (c) Schematic of the phase transition. At a small reduced Coulomb temperature or equivalently high ionic interaction, the system is fully paired. Otherwise, there are some remaining free ions. (d) (Red points) Free ion fraction from BD simulations for various reduced Coulomb temperatures. (Red line) Theoretical curve for $r_0 = 1.2$ nm and $\zeta = 0.22$. (Green points) Free charge carrier density from MD simulations for various reduced Coulomb temperatures. (Green line) Theoretical curve for $r_0 = 0.18$ nm and $\zeta = 0.33$.

We find $T_c^* = 0.17$, which is very close to the theoretical value $T_c^* = 0.18$. The comparison between theory and simulations notably confirms that the correlation length does diverge in a non-algebraic way close to the transition, validating the fact it is of infinite order. The comparison between the fraction of free ions in simulations and theory [see Eq. (12)] shows similarly good agreement, as displayed in Fig. 2(d) (red symbols and solid line).

2. Molecular dynamics simulations and effect of the short-range interactions

In Sec. III B 1, we discussed BD simulations where ions do not have any repulsion potential, meaning that short-distance structures could be adequately resolved. Without repulsive potential, the distance between ions in a pair fluctuates around 0. As there is no permanent dipole in this case, their interactions with other ions are very weak. In all atom MD, where ions also interact through repulsive LJ interactions, pairs fluctuate around a finite distance [see Figs. 1(b) and 2(b)]. In this case, interactions with pairs are no longer negligible, allowing the formation of more complex structures.

Other works[14,19] that used different simulation techniques reported various possible structures of ionic clusters, depending, for example, on the chemical nature of ions[14,19] or the wall.[20] In our case, ion correlation functions reveal a short-distance structuration due to contact and solvent-separated ion binding, up to clusters of size ∼6 in the absence of electric fields (Fig. S3). Overall, the relations between short-range interaction and short-range structure seem non-universal and are, in practice, difficult to analyze. Instead, we can focus on the free ion fraction, in comparison with BD simulations.

We find that like in BD, the free ion fraction n_f drops to zero below a critical temperature, as shown in Fig. 2(d) (green symbols). The behavior of n_f with temperature is well-described by theoretical predictions; however, the value of the critical temperature is found to differ from BD simulations, with $T_c^* \simeq 0.24$. This discrepancy can be attributed to two facts. First, in MD simulations, we only account for a single layer of wall atoms: the electrolyte is thus effectively confined by a slab of empty space, with $\epsilon_r = 1$, leading to a much higher value of the dielectric length $\xi = 28$ nm. In addition, the minimal inter-ion approach distance is now unequivocally set by the physical size of ions, set by Lennard–Jones short-distance interactions. For our choice of simulation parameters, the distance of physical contact is $r_0 = 0.18$ nm (corresponding to approximately twice the ionic radius of sodium). For these values of ξ and r_0, we obtain from our theoretical model $T_c^* = 0.24$, very close to the value inferred from simulations [Fig. 2(d), green line.]

To obtain the theoretical curves of Fig. 2(d), one must also specify the quantity denoted ζ in Eq. (12). It can be interpreted as a "volume fraction": if one fixes the position of the first ion (assumed to be a disk of radius $r_0/2$), one must place the second ion exactly at a distance r_0 from the first ion's center to form a contact pair. Within that disk of radius r_0, the pair occupies a fraction $\zeta_{\mathrm{MD}} \simeq 0.36$ (corresponding to the central ion and around half of the second one). If instead ions are allowed to overlap, as in BD, then that fraction drops to approximately $\zeta_{\mathrm{BD}} \simeq 0.25$ as paired ions almost fully overlap. In practice, we treat ζ as a fitting parameter for the sake of simplicity and obtain $\zeta_{\mathrm{MD}} = 0.33$ and $\zeta_{\mathrm{BD}} = 0.22$, very close to estimated values.

Similarly, we show in the supplementary material that the fraction of charged clusters also exhibits a drop below T_c^*. However, we find that the equilibration time of clusters grows rapidly as the temperature is lowered: due to our limited simulation time, we find that n_f^{cluster} is not exactly zero at very low temperature.

It should be noted that in our theory, the chemical equilibrium [Eq. (12)] should, in principle, be updated to take the formation of clusters into account, instead of only ion pairs. In practice, however, large clusters only represent a small fraction of ions (see Fig. S3), and Eq. (12) can be used as an approximation.

IV. NON-LINEAR TRANSPORT

In this section, we study the out-of-equilibrium properties of the 2D confined systems under electric driving. In particular, we focus on the increase in conductivity caused by the field-induced dissociation of ion pairs, a process known as the second Wien effect. We show analytically that this phenomenon is at the source of the non-linear ion transport as the ionic current across the nanofluidic slit becomes a power law of the applied voltage, with a non-universal exponent, different from the 3D case. Brownian dynamics validate these theoretical predictions and notably the strong dependence of the exponent with the reduced Coulomb temperature.

A. Non-linear behavior of the ionic current

As previously stated, the application of an external electric field across the 2D slit tends to break ion pairs, effectively increasing the electrolyte's conductivity. Numerically, we can quantify this non-linear contribution by subtracting from the total ionic current, the Ohmic term resulting from the conduction of ions that are free in the absence of field,

$$\delta j(E) \simeq j(E) - n_f(0) j_0 = \delta n_f(E) j_0, \tag{26}$$

with $j_0 = \sigma_0 E$ being the current density of a fully dissociated electrolyte. In terms of conductivity, this yields the following contributions:

$$\sigma(E) = \sigma_0 + \delta\sigma(E). \tag{27}$$

Figure 3(a) shows the conductivity as a function of the electric field below and above the transition. When $E \to 0$, we observe that the conductivity tends linearly to a constant above the transition $T^* > T_c^*$ and vanishes like a power law below the transition. In this regime, we will define the exponent $\alpha(T^*)$,

$$|\delta j(E)| \underset{E\to 0}{\propto} |E|^{\alpha(T^*)}. \tag{28}$$

In the limit of large applied fields, we instead observe that $n_f \to 1$: we recover Ohm-like conduction as in fully dissociated electrolytes. The corresponding ionic current I is plotted in Fig. 4(b).

B. Theory

In this section, we analytically derive the expression of the non-universal exponent $\alpha(T^*)$. Our approach is based on an extension of Onsager's study of the second Wien effect for bulk 3D weak electrolytes.[33] The generalization to 2D has been first developed in Ref. 14, and we elaborate on this description here to compare with

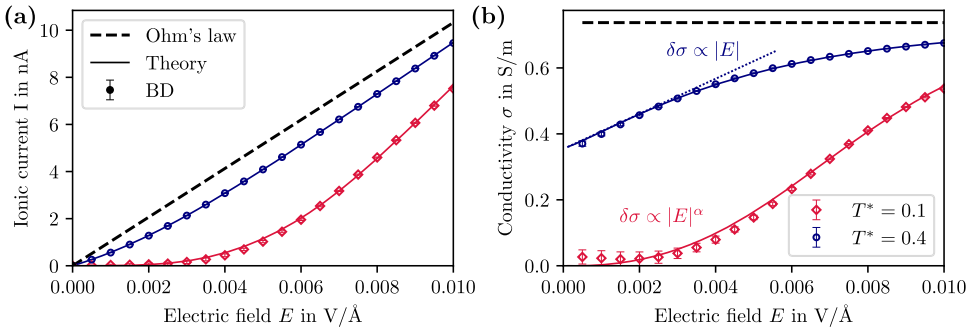

FIG. 3. Comparison between BD transport simulations and theory. [(a) and (b)] Ionic current (a) and conductivity (b) for reduced Coulomb temperature of 0.1 (red) and 0.4 (blue), compared with Ohm's law (dashed black line). Symbols: BD simulations. Solid lines: theoretical model, Eq. (61).

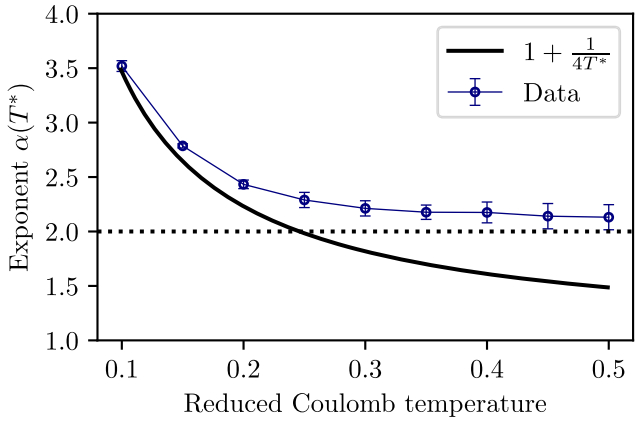

FIG. 4. Symbols: exponent α defined by the non-linearity in the IV curve, $|j(E)| \propto |E|^\alpha$. Black solid line: theoretical prediction of the 2D Wien effect [see Eq. (63)]. Dotted line: bulk exponent $\alpha = 2$, obtained through Onsager's theory of the Wien effect.[33]

our numerical results. In what follows, we restrict ourselves to the case of the ideal 2D Coulomb gas ($\xi = \infty$) and focus on the paired regime, ($T^* < T_c^*$).

1. An Onsager's approach of the 2D Wien effect

We assume that the fraction n_f follows a generic evolution equation, introducing a dissociation (respectively, association) time τ_d (respectively, τ_a),

$$\dot{n}_f = \frac{1 - n_f}{\tau_d} - \frac{n_f^2}{\tau_a}. \tag{29}$$

At thermal equilibrium (in the absence of an external field), the ratio of these two times is given by $e^{2\mu_\epsilon}$, as discussed in Sec. III A. When driven out of equilibrium, however, these two quantities may depend on the applied electric field $\mathbf{E} = E\,\hat{\mathbf{x}}$ acting along x.

Onsager showed that it is possible to link both τ_a and τ_d to the anion–cation correlation function g. Assuming that a cation is held fixed at the origin, $g(r, \theta)$ is the probability density of finding a negative ion at the polar position (r, θ). It follows a Smoluchowski equation,

$$\partial_t g = 2D\nabla \cdot (\nabla g + g\nabla V), \tag{30}$$

where V is the total (dimensionless) electrostatic potential at (r, θ). It reads

$$V = \frac{1}{T^*} \log \frac{r}{r_0} - \frac{r \cos\theta}{\ell_E}. \tag{31}$$

Here, we made the approximation that $\log r/(r + \xi) \sim \log r$, which is reasonable for $r < \xi$. Since $\xi = 14$ nm, this approximation is valid over the typical length scales of ionic correlations. The first term of the potential corresponds to the unscreened interaction of two ions in confinement. This assumption is valid if the system is sufficiently paired up ($T^* < T_c^*$) so that the influence of other free ions can be neglected. Quantitatively, the Debye length λ_D diverges if the system is fully paired and, therefore, is not a relevant length scale. The second term corresponds to the external field, characterized by the following length scale,

$$\ell_E = \frac{k_B T}{Ze|E|}. \tag{32}$$

The potential V has a maximum for $r \sim \ell_E/T^*$; a pair can be expected to break if its two ions are separated by a larger distance. This fixes the typical length scale of correlations in the presence of the field.

Assuming the system has reached a steady state, we obtain

$$\left[\Delta + \left(\frac{1}{T^* r} - \frac{\cos\theta}{\ell_E}\right)\partial_r + \frac{\sin\theta}{r\ell_E}\partial_\theta\right] g = 0. \tag{33}$$

We then perform the change of variable $\mathbf{r} \to \mathbf{u} = \mathbf{r}/\ell_E$,

$$\left[\Delta + \left(\frac{1}{T^* u} - \cos\theta\right)\partial_u + \frac{\sin\theta}{u}\partial_\theta\right] g = 0. \tag{34}$$

This shows that the problem is scale invariant as it is now entirely determined by a single dimensionless parameter T^*; this property is unique to the 2D geometry (where the Bjerrum length is infinite). Onsager's trick consists in splitting the correlation function into two parts,

$$g = g_d + g_a, \tag{35}$$

where g_d and g_a are two solutions of (34) associated with a source or a sink of particles at the origin, respectively,

$$\int_0^{2\pi} -2D[\nabla g_a + g_a \nabla V] \cdot \hat{\mathbf{r}}\, r d\theta = -C, \tag{36}$$

$$\lim_{r\to\infty} g_a = \rho, \tag{37}$$

and

$$\int_0^{2\pi} -2D\left[\nabla g_d + g_d \nabla V\right]\cdot \hat{\mathbf{r}}\, r\mathrm{d}\theta = +C, \tag{38}$$

$$\lim_{r\to\infty} g_d = 0, \tag{39}$$

where C is a positive constant independent of r and ρ is the average ionic density far from the central ion. In other words, g_a describes a background of free ions recombining with the central ion to form new pairs and g_d pairs that break under the electric field. These two functions will allow us to compute τ_a and τ_d.

Since any constant is a solution of the Smoluchowski equation, it is easy to see from the boundary condition that

$$g_a = \rho, \tag{40}$$

and straightforward integration yields

$$C = \frac{4\pi D\rho}{T^*}. \tag{41}$$

This is a recombination rate, defining the pair association time,

$$\tau_a = \frac{T^*}{4\pi D\rho}. \tag{42}$$

Interestingly, we find that the formation time of pairs is independent of the electric field. This result is general and is also valid in the bulk (but not in 1D), as the recombination of freely diffusive ions is an uncorrelated process.

Onsager's original approach to compute g_d, which involves an arduous expansion in terms of special functions, strongly relied on the fact that the 3D Smoluchowski equation is spatially separable; it fails in our 2D case. Instead, we exploit the fact that the 2D Smoluchowski equation is scale-invariant and show how all relevant quantities can be computed up to a geometrical factor.

2. Self-similarity of the correlation function

We start by noticing that another solution of the Smoluchowski equation (34) is the Boltzmann distribution,

$$g_0(u,\theta) = \exp\left[-\frac{1}{T^*}\ln\frac{u\ell_E}{r_0} + u\cos\theta\right]. \tag{43}$$

This is not the correct solution to the problem, however, as the Boltzmann distribution only makes sense at thermal equilibrium. In particular, it does not verify the correct boundary conditions at $r\to\infty$. However, for $u \ll 1$, the external field is negligible compared to the field created by the central ion and pairs are in quasi-equilibrium (ions are strongly correlated and remain bounded over long timescales). Therefore, the total correlation function g should diverge like g_0 for $u\to 0$. Since g_a is bounded around $u=0$, this condition also provides us a boundary condition for g_d, which is therefore the solution of

$$\left[\Delta + \left(\frac{1}{T^* u} - \cos\theta\right)\partial_u + \frac{\sin\theta}{u}\partial_\theta\right] g_d = 0, \tag{44}$$

$$g_d \sim K_a\left(\frac{\ell_E}{r_0}\right)^{-1/T^*} u^{-1/T^*} \quad \text{for } u\to 0, \tag{45}$$

$$\lim_{u\to\infty} g_d(u) = 0, \tag{46}$$

where K_a is a constant determined by the fact that the flux of g_d should be equal to $+C$. The solution to this problem is unique because g_d is known on the whole boundary of the domain. ℓ_E now only appears in a boundary condition at $u=0$, and the system is linear, so g_d is fully determined from a single scaling function,

$$g_d(u) = K_a\left(\frac{l_E}{r_0}\right)^{-1/T^*} G(u), \tag{47}$$

where G is a function that depends only on T^*. The balance between the fluxes of g_d and g_a reads

$$2DK_a\left(\frac{\ell_E}{r_0}\right)^{-1/T^*} \mathcal{F} = \frac{4\pi D\rho}{T^*}, \tag{48}$$

where $\mathcal{F}$ is the flux of the function G,

$$\mathcal{F} = -\int_0^{2\pi} \left[\nabla G + G\nabla\hat{V}\right]\cdot\hat{\mathbf{u}}\, u\mathrm{d}\theta, \tag{49}$$

where the dimensionless potential $\hat{V}$ is given by

$$\hat{V} = \frac{1}{T^*}\log u - u\cos\theta. \tag{50}$$

The flux $\mathcal{F}$ has the dimension of an inverse length squared and is independent of ℓ_E or ρ since it describes a single pair breaking event. As the only remaining length scale in the problem is r_0, we have (up to a geometrical factor)

$$\mathcal{F} \simeq r_0^{-2}. \tag{51}$$

We obtain the association constant K_a,

$$K_a = 2\pi\left(\frac{\ell_E}{r_0}\right)^{1/T^*} \frac{\rho r_0^2}{T^*} = \frac{\tau_d}{\tau_a}, \tag{52}$$

and the dissociation time τ_d,

$$\tau_d = \frac{r_0^2}{2D}\left(\frac{\ell_E}{r_0}\right)^{1/T^*}. \tag{53}$$

In the steady state, the free ion fraction n_f is given by Eq. (29),

$$n_f = \frac{\tau_a}{2\tau_d}\left(\sqrt{1+\frac{4\tau_d}{\tau_a}} - 1\right). \tag{54}$$

It should be noted that this result is general for any system with Onsager's pairing kinetics and does not depend on details of ionic interactions as long as τ_a and τ_d are known. In the limit of a weak applied field, $\tau_d \gg \tau_a$ and $n_f \ll 1$. We obtain

$$n_f \simeq \sqrt{\frac{\tau_a}{\tau_d}}, \tag{55}$$

with τ_a and τ_d given by Eqs. (42) and (53), respectively. Assuming each free ion contributes linearly to conduction, $j(E) \propto E \times n_f(E)$ and we obtain the ionic current due to the Wien effect,

$$|j(E)| \propto |E|^{1+1/2T^*}. \tag{56}$$

This predicts there that the ionic conductivity scales sublinearly with the temperature as $\sigma \sim |E|^{1/2T^*}$. While this prediction qualitatively reproduces the non-linearity observed in the simulations, it typically underestimates the conductivity of the system by more than one order of magnitude. In particular, we do not find the exponent measured in the simulations.

In Sec. IV B 3, in order to explain this behavior, we now take into account the formation of larger ionic clusters in the presence of an external field. We do so by first rederiving our result through scaling arguments and then amending it using the same scaling logic.

Finally, the above derivation critically relies on the (quasi-) logarithmic shape of the interaction potential: because its typical length scale ξ is much larger than any other physical length scale in the problem, ionic correlations become self-similar. This situation is unique to the 2D case; for example, in bulk electrolytes, ions interact through the usual $1/r$ Coulomb's law (which has a typical length scale set by the Bjerrum length ℓ_B, see Sec. III A 2) and computing correlations is much more mathematically involved.[33]

3. Scaling laws and anisotropic conduction

In the above derivation, the key assumption was the divergence of the Debye length λ_D so that the problem becomes self-similar. We recall that $\lambda_D \propto n_f^{-1/2}$, and we found that $n_f \propto E^{1/2T^*}$ so that $\lambda_D \propto E^{-1/4T^*}$. If $T^* < 1/4$, then $\lambda_D \gg \ell_E$ for all relevant values of the electric field since $\ell_E \propto E^{-1}$.

This scaling argument seemingly validates our approach of considering that ℓ_E sets the scale of all correlations between ions. However, this argument only makes sense when considering correlations along the x axis: ions separated by more than ℓ_E are carried away by the electric field, so correlations on larger scale may be neglected. This is not the case, however, along the y axis, so actually one should not neglect the influence of λ_D on the problem: correlations are anisotropic.

The above analysis can be supported qualitatively by analyzing simulation results. In Brownian dynamics, we observe that ions tend to form elongated clusters in the direction of the electric field. Ions are able to move within these clusters but remain within them for long time (see Fig. S3). This suggests that the mobility of ions in the direction x of the electric field may increase with the field strength, while diffusion in the orthogonal direction y remains constrained by electrostatic correlations.

Taking anisotropic correlations into account, however, requires to account for many-body interactions in the Smoluchowski equation for g, which makes the problem intractable. Instead, we use a scaling argument, which we now detail.

Let us start by recovering the previous result using scaling laws. Equation (53) can be recast as an Arrhenius law,

$$\tau_d = \tau_{\text{diffusion}} \exp\left[-2\beta\Delta F\right] = \frac{r_0^2}{2D}\left(\frac{\ell_E}{r_0}\right)^{1/T^*}, \tag{57}$$

where ΔF is the "free energy barrier" to break a pair. It reads

$$\beta\Delta F \simeq -\frac{\log \ell_E/r_0}{2T^*}. \tag{58}$$

This argument is not fully rigorous as the problem is far from equilibrium, and this energy barrier strongly depends on an out-of-equilibrium quantity (the length scale ℓ_E). However, this last expression is identical, upon replacing ℓ_E by λ_D to the (properly defined) free energy cost of breaking a pair at equilibrium, given by Eq. (23). We, thus, find that the *kinetic* energy barrier to break a pair is similar to the *thermodynamic* energy gap between the paired and the unpaired states if we admit that the typical size of the ionic atmosphere in the presence of an external field is given by ℓ_E instead of the Debye length λ_D.

Let us now use this simple argument to account for anisotropic correlations. Since the typical size of the correlation cloud is ℓ_E along the x axis and λ_D along the y axis, one may roughly approximate its overall spatial extension as $\ell = \sqrt{\lambda_D \ell_E}$. In this case, the free energy barrier to breaking a pair should read

$$\beta\Delta F \simeq -\frac{\log \ell_E/r_0}{4T^*} - \frac{\log \lambda_D/r_0}{4T^*} \tag{59}$$

so that it is now the sum of two terms, corresponding to the energy barrier that an ion has to overcome to escape a cluster in the x or y direction, respectively. Conduction in the direction of the field is therefore associated with the Arrhenius timescale corresponding to the first term in the free energy,

$$\tau_{d,x} = \frac{r_0^2}{2D}\left(\frac{\ell_E}{r_0}\right)^{1/2T^*}, \tag{60}$$

and we can define the proportion n_x of ions that can freely move along the x axis. It follows an evolution equation similar to Eq. (29), with $\tau_{d,x}$ replacing τ_d. We obtain

$$n_x = \frac{\tau_a}{2\tau_{d,x}}\left(\sqrt{1+\left(\frac{2\tau_{d,x}}{\tau_a}\right)^2} - 1\right) \underset{E\to 0}{\propto} E^{1/4T^*}. \tag{61}$$

We finally obtain the following prediction for the total ionic current,

$$|j(E)| \propto |E| \times n_x(E) \propto \times |E|^{\alpha(T^*)}, \tag{62}$$

with

$$\alpha(T^*) = 1 + \frac{1}{4T^*}. \tag{63}$$

4. Comparison with simulations and discussion

The comparison between our BD simulations and Eq. (62) is plotted in Figs. 4(a) and 4(b). Below the Kosterlitz–Thouless transition, the agreement is quantitative and the observed exponent $\alpha(T^*)$ in simulations matches the theoretical prediction. Conductivity scales like

$$\text{For } T^* < T_c, \quad \sigma(E) \propto |E|^{\alpha-1}, \quad \alpha \simeq 1 + \frac{1}{4T^*}. \tag{64}$$

Interestingly, this exponent is non-universal as it strongly depends on temperature; this contrasts with bulk electrolytes where the

second Wien effect results in a universal conductivity increment scaling, such as $\delta\sigma \propto |E|$

Above the pairing transition, however, we observe deviations to the law. We find that the conductivity increases linearly with the applied field [Fig. 3(b)], which echoes the bulk Wien effect as mentioned above. We now suggest a possible explanation.

The key element in the above derivation that led to the non-universal exponent $1/4T^*$ was the self-similarity of the correlation function. Below the KT transition, this assumption is valid as almost all ions are paired up, resulting in a diverging correlation function for electrostatic correlations: $\lambda_D \to \infty$. However, for $T^* > T_c$, some free ions remain even for $E = 0$, and λ_D always remains finite. Therefore, the correlation function is not self-similar as the problem now possesses two typical length scales: λ_D and ℓ_E. The second Wien effect may then be obtained from scaling laws: in the absence of field, an ion pair breaks when its two ions are separated by more than λ_D (after which they cease to interact). Under an electric field, this transition state between pairs and free ions is destabilized by roughly a factor $\lambda_D/\ell_E \propto |E|$. Since the dissociation timescale is approximatively the Arrhenius time associated with this intermediate state, conductivity also increases by a factor linear in $|E|$: we recover the scaling of Onsager's Wien effect in bulk electrolytes. We, therefore, obtain

$$\text{For } T^* > T_c, \quad \sigma(E) - \sigma(0) \propto |E|^{\alpha-1}, \quad \alpha \simeq 2, \qquad (65)$$

in good agreement with numerical simulations (Fig. 4).

It should be noted, however, that in the bulk, the remaining free ions at $E = 0$ do not play a significant role at sufficient dilution because $\lambda_D > \ell_B$ and so correlations still have a typical length scale ℓ_B. In other words, the conductivity increment will scale like E at all temperatures and does not directly depend on ion concentration, unlike in confined electrolytes.

The above derivation was performed assuming that all ions are paired up. In what follows, we account for ions that remain free even in the absence of any field by adding a contribution $n_f(0)$ to the above result; this term is determined by the procedure described in the supplementary material. Sections IV B 1–IV B 3 were dedicated to the theoretical analysis of the 2D Wien effect at low temperature ($T^* < T_c^*$). We find that the conductivity of 2D confined electrolytes evolves as a power law of the electric field, with a non-universal exponent $1/4T^*$. This contrasts with the 3D bulk case, where the Wien exponent is 1.

Finally, we note that in both cases $T^* > T_c$ and $T^* < T_c$, the exponent cannot be found through simple symmetry arguments, which would dictate that $\sigma \propto E^2$ (as the system is invariant by reversing the direction of the electric field). This originates in the fact that the correlation function g becomes strongly polarized in the direction of the field, breaking the $x \to -x$ symmetry. In the bulk case, the conductivity increment scales like the ratio $\ell_B/\ell_E \propto E$, with ℓ_B being the Bjerrum length. Since this quantity is infinite in 2D, the problem becomes self-similar and the increment is found to scale like a non-universal power law.

V. CONCLUSION

In this paper, we investigate the effect of long range electrostatic correlations on the equilibrium and transport of ions confined in a 2D slit. We use a combination of molecular dynamics simulations, analytical theory, and Brownian dynamics (where water and channel walls are treated implicitly and ion–ion interactions are renormalized). In all cases, we find that 2D confinement results in stronger electrostatic interactions, leading to the formation of ionic pairs. We showed that this phenomenon is associated with a phase transition analogous to the Kosterlitz–Thouless transition and suppresses linear ionic conduction at low temperature.

In addition, the application of an external field can result in the breaking of ion pairs and an increase in conduction. This process, known as the Wien effect, leads to strongly non-linear ion transport under confinement.

We expect that the effective potential approach used in this paper could be extended to explore other materials[10] but also other geometries, for example, the case of multiple ionic layers,[34] by changing the effective interaction potential accordingly. Models of ionic cluster dynamics are also useful to study ionic liquids, where many parallels can be drawn for the relations between ion correlations and transport phenomena.[35]

Overall, we obtain excellent agreement between our analytical models and numerical results for both the pairing transition and the second Wien effect. In particular, we find that in the pair-dominated regime, the ionic current behaves like a power law of the applied field, with a non-universal exponent that can be predicted from analytical field theories. This regime, where the conductivity strongly vanishes at low electric field, can be considered as the ionic coulomb blockade situation—although no gating dependence is considered here.

This work is also a further demonstration of the very particular nature of electrostatic interactions in confined geometry. The strong ionic correlations give rise to a complex variety of structures and behaviors, but the large-scale picture remains unaffected and can be adequately understood in terms of a small set of parameters. Consequently, this work sheds light on the structure of ion–ion correlations in confined systems and on the ionic dynamics of nanofluids in general.

Finally, the emergence of strongly non-linear conduction effects in 2D is a richness, which can be exploited to develop nanofluidic systems with advanced properties, such as memristors.[11,13] This is an opportunity that will certainly result in further developments in this active domain.[36–38]

SUPPLEMENTARY MATERIAL

The supplementary material includes details of numerical simulations, including the values of all numerical parameters. We also detail the procedures to accurately extract the average number of pairs from numerical correlation functions, as well as the IV curve exponent α.

ACKNOWLEDGMENTS

The authors thank B. Coquinot and G. Monet for fruitful discussions. L.B. acknowledges support from ERC-Synergy Grant Agreement No. 101071937, n-AQUA. P.R. acknowledges support from the European Union's Horizon 2020 research and innovation program under Marie Sklodowska-Curie Grant Agreement No. 101034413.

AUTHOR DECLARATIONS

Conflict of Interest

The authors have no conflicts to disclose.

Author Contributions

Damien Toquer: Data curation (lead); Formal analysis (lead); Investigation (equal); Methodology (lead); Visualization (lead); Writing – original draft (equal); Writing – review & editing (equal). **Lydéric Bocquet**: Conceptualization (equal); Funding acquisition (equal); Supervision (equal); Validation (equal); Writing – review & editing (equal). **Paul Robin**: Conceptualization (equal); Formal analysis (equal); Investigation (equal); Supervision (equal); Validation (equal); Writing – original draft (equal); Writing – review & editing (equal).

DATA AVAILABILITY

The data that support the findings of this study are available from the corresponding author upon reasonable request.

REFERENCES

[1]L. Bocquet and E. Charlaix, "Nanofluidics, from bulk to interfaces," Chem. Soc. Rev. **39**, 1073–1095 (2010).
[2]S. Garaj, W. Hubbard, A. Reina, J. Kong, D. Branton, and J. A. Golovchenko, "Graphene as a subnanometre trans-electrode membrane," Nature **467**, 190–193 (2010).
[3]C. Y. Lee, W. Choi, J.-H. Han, and M. S. Strano, "Coherence resonance in a single-walled carbon nanotube ion channel," Science **329**, 1320–1324 (2010).
[4]J. Feng, M. Graf, K. Liu, D. Ovchinnikov, D. Dumcenco, M. Heiranian, V. Nandigana, N. R. Aluru, A. Kis, and A. Radenovic, "Single-layer MoS_2 nanopores as nanopower generators," Nature **536**, 197–200 (2016).
[5]E. Secchi, S. Marbach, A. Niguès, D. Stein, A. Siria, and L. Bocquet, "Massive radius-dependent flow slippage in carbon nanotubes," Nature **537**, 210–213 (2016).
[6]B. Radha, A. Esfandiar, F. C. Wang, A. P. Rooney, K. Gopinadhan, A. Keerthi, A. Mishchenko, A. Janardanan, P. Blake, L. Fumagalli, M. Lozada-Hidalgo, S. Garaj, S. J. Haigh, I. V. Grigorieva, H. A. Wu, and A. K. Geim, "Molecular transport through capillaries made with atomic-scale precision," Nature **538**, 222–225 (2016).
[7]A. Esfandiar, B. Radha, F. C. Wang, Q. Yang, S. Hu, S. Garaj, R. R. Nair, A. K. Geim, and K. Gopinadhan, "Size effect in ion transport through angstrom-scale slits," Science **358**, 511–513 (2017).
[8]N. Kavokine, R. R. Netz, and L. Bocquet, "Fluids at the nanoscale: From continuum to subcontinuum transport," Annu. Rev. Fluid Mech. **53**, 377–410 (2021).
[9]N. Kavokine, S. Marbach, A. Siria, and L. Bocquet, "Ionic Coulomb blockade as a fractional Wien effect," Nat. Nanotechnol. **14**, 573–578 (2019).
[10]N. Kavokine, P. Robin, and L. Bocquet, "Interaction confinement and electronic screening in two-dimensional nanofluidic channels," J. Chem. Phys. **157**, 114703 (2022).
[11]P. Robin and L. Bocquet, "Nanofluidics at the crossroads," J. Chem. Phys. **158**, 160901 (2023).
[12]L. A. Richards, A. I. Schäfer, B. S. Richards, and B. Corry, "The importance of dehydration in determining ion transport in narrow pores," Small **8**, 1701–1709 (2012).
[13]P. Robin, T. Emmerich, A. Ismail, A. Niguès, Y. You, G.-H. Nam, A. Keerthi, A. Siria, A. Geim, B. Radha, and L. Bocquet, "Long-term memory and synapse-like dynamics in two-dimensional nanofluidic channels," Science **379**, 161–167 (2023).
[14]P. Robin, N. Kavokine, and L. Bocquet, "Modeling of emergent memory and voltage spiking in ionic transport through angstrom-scale slits," Science **373**, 687–691 (2021).
[15]T. Emmerich, K. S. Vasu, A. Niguès, A. Keerthi, B. Radha, A. Siria, and L. Bocquet, "Enhanced nanofluidic transport in activated carbon nanoconduits," Nat. Mater. **21**, 696–702 (2022).
[16]Y. Levin, "Electrostatic correlations: From plasma to biology," Rep. Prog. Phys. **65**, 1577–1632 (2002).
[17]P. Minnhagen, "The two-dimensional Coulomb gas, vortex unbinding, and superfluid-superconducting films," Rev. Mod. Phys. **59**, 1001–1066 (1987).
[18]P. Robin, A. Delahais, L. Bocquet, and N. Kavokine, "Ion filling of a one-dimensional nanofluidic channel in the interaction confinement regime," J. Chem. Phys. **158**, 124703 (2023).
[19]W. Zhao, Y. Sun, W. Zhu, J. Jiang, X. Zhao, D. Lin, W. Xu, X. Duan, J. S. Francisco, and X. C. Zeng, "Two-dimensional monolayer salt nanostructures can spontaneously aggregate rather than dissolve in dilute aqueous solutions," Nat. Commun. **12**, 5602 (2021).
[20]K. Fong, B. Sumic, N. O'Neill, C. Schran, C. Grey, and A. Michaelides, "The interplay of solvation and polarization effects on ion pairing in nanoconfined electrolytes," Nano Lett. **24**, 5024 (2024).
[21]Y. Avni, R. M. Adar, D. Andelman, and H. Orland, "Conductivity of concentrated electrolytes," Phys. Rev. Lett. **128**, 098002 (2022).
[22]L. Fumagalli, A. Esfandiar, R. Fabregas, S. Hu, P. Ares, A. Janardanan, Q. Yang, B. Radha, T. Taniguchi, K. Watanabe, G. Gomila, K. S. Novoselov, and A. K. Geim, "Anomalously low dielectric constant of confined water," Science **360**, 1339–1342 (2018).
[23]A. Schlaich, E. W. Knapp, and R. R. Netz, "Water dielectric effects in planar confinement," Phys. Rev. Lett. **117**, 048001 (2016).
[24]G. Monet, F. Bresme, A. Kornyshev, and H. Berthoumieux, "Nonlocal dielectric response of water in nanoconfinement," Phys. Rev. Lett. **126**, 216001 (2021).
[25]R. Wang, M. Souilamas, A. Esfandiar, R. Fabregas, S. Benaglia, H. Nevison-Andrews, Q. Yang, J. Normansell, P. Ares, G. Ferrari *et al.*, "In-plane dielectric constant and conductivity of confined water," arXiv:2407.21538 (2024).
[26]C. C. Rochester, A. A. Lee, G. Pruessner, and A. A. Kornyshev, "Interionic interactions in conducting nanoconfinement," ChemPhysChem **14**, 4121–4125 (2013).
[27]S. Kondrat, N. Georgi, M. V. Fedorov, and A. A. Kornyshev, "A superionic state in nano-porous double-layer capacitors: Insights from Monte Carlo simulations," Phys. Chem. Chem. Phys. **13**, 11359–11366 (2011).
[28]V. Kaiser, "The Wien effect in electric and magnetic Coulomb systems—From electrolytes to spin ice," Ph.D. thesis, Ecole normale supérieure de lyon - ENS LYON, 2014.
[29]V. Kaiser, S. T. Bramwell, P. C. W. Holdsworth, and R. Moessner, "Onsager's Wien effect on a lattice," Nat. Mater. **12**, 1033–1037 (2013).
[30]H. Berthoumieux, V. Démery, and A. C. Maggs, "Non-monotonic conductivity of aqueous electrolytes: Beyond the first Wien effect," J. Chem. Phys. **161**, 184504 (2024).
[31]B. Rotenberg, O. Bernard, and J.-P. Hansen, "Underscreening in ionic liquids: A first principles analysis," J. Phys.: Condens. Matter **30**, 054005 (2018).
[32]N. Bjerrum, *Untersuchungen Über Ionenassoziation. I. Der Einfluss Der Ionenassoziation Auf Die Aktivität Der Ionen Bei Mittleren Assoziationsgraden* (B. Lunos, 1926).
[33]L. Onsager, "Deviations from Ohm's law in weak electrolytes," J. Chem. Phys. **2**, 599–615 (1934).
[34]B. Coquinot, M. Becker, R. R. Netz, L. Bocquet, and N. Kavokine, "Collective modes and quantum effects in two-dimensional nanofluidic channels," Faraday Discuss. **249**, 162–180 (2024).
[35]G. Feng, M. Chen, S. Bi, Z. A. Goodwin, E. B. Postnikov, N. Brilliantov, M. Urbakh, and A. A. Kornyshev, "Free and bound states of ions in ionic liquids, conductivity, and underscreening paradox," Phys. Rev. X **9**, 021024 (2019).
[36]T. M. Kamsma, J. Kim, K. Kim, W. Q. Boon, C. Spitoni, J. Park, and R. van Roij, "Brain-inspired computing with fluidic iontronic nanochannels," Proc. Natl. Acad. Sci. U. S. A. **121**, e2320242121 (2024).
[37]T. Emmerich, Y. Teng, N. Ronceray, E. Lopriore, R. Chiesa, A. Chernev, V. Artemov, M. Di Ventra, A. Kis, and A. Radenovic, "Nanofluidic logic with mechano–ionic memristive switches," Nat. Electron. **7**, 271–278 (2024).
[38]G. Paulo, K. Sun, G. Di Muccio, A. Gubbiotti, B. Morozzo della Rocca, J. Geng, G. Maglia, M. Chinappi, and A. Giacomello, "Hydrophobically gated memristive nanopores for neuromorphic applications," Nat. Commun. **14**, 8390 (2023).